

Cyclic Azacyanines: Experimental and Computational Studies on Spectroscopic Properties and Unique Reactivity

Digambara Patra · Teresa A. Palazzo ·
Nagham N. Malaeb · Makhluf J. Haddadin ·
Dean J. Tantillo · Mark J. Kurth

Received: 1 April 2014 / Accepted: 19 May 2014 / Published online: 10 June 2014
© Springer Science+Business Media New York 2014

Abstract The absorption and fluorescence properties of cyclic azacyanine (**CAC**) derivatives were examined in several solvents. The presence of electron donating or withdrawing groups on the **CAC** impacts spectroscopic properties. The general solvent relaxation displayed by azacyanine derivatives is in accordance with Lippert-Mataga's prediction but exception is noted in the case of protic solvent due to specific hydrogen bonding interactions. Fluorescence lifetime decay studies indicate a relaxation time in the nanosecond timescale with mono exponential decay. Donating substituents markedly increase the excited state lifetime, whereas withdrawing groups marginally decrease the excited state lifetime. Quantum chemical computations were used to explore the origins of the reactivity and spectroscopic properties of **CACs**; results are consistent with a model in which regioselectivity results from differences in mechanistic steps occurring after initial attack by hydroxide on the **CAC**.

Keywords Cyclic Azacyanine · Solvent effect · Fluorescence · Excited State · Computational Chemistry

Electronic supplementary material The online version of this article (doi:10.1007/s10895-014-1413-0) contains supplementary material, which is available to authorized users.

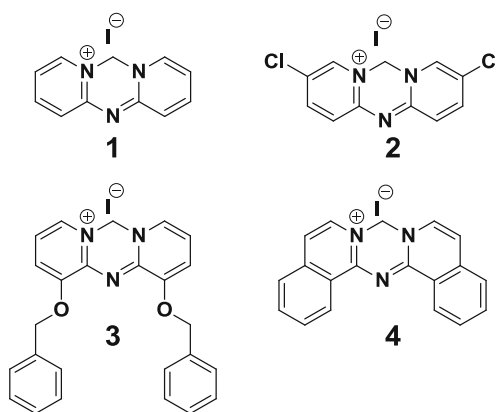
D. Patra (✉) · N. N. Malaeb · M. J. Haddadin
Department of Chemistry, American University of Beirut, Beirut,
Lebanon
e-mail: dp03@aub.edu.lb

T. A. Palazzo · D. J. Tantillo (✉) · M. J. Kurth (✉)
Department of Chemistry, University of California, One Shields
Avenue, Davis, CA 95616, USA
e-mail: djtantillo@ucdavis.edu
e-mail: mjkurth@ucdavis.edu

Introduction

Cyclic azacyanine (**CAC**) derivatives have recently been reported to have intriguing spectroscopic and fluorescence properties [1]. The fluorescence properties of such molecules are influenced by both positional substitution and solvent environment. In general, fluorescence and optical properties of cyanine dyes are of importance as they are widely used to enhance the sensitivity range of photographic emulsions in their ability to form images on film [2–4]. Currently, these dyes are also receiving attention as fluorophores for applications in biomedical imaging [5–7], single molecule studies [8–11] and Fluorescence Correlation Spectroscopy (FCS) [12]. For such biomedical applications, the fluorescence response of the probe molecule with variation in local environment and/or polarity of the sample is crucial. Solvent environment exerts a strong influence on chemical equilibria, reaction rates, and electronic spectra (position and intensity) [13].

Because the spectral properties of a chemical species are influenced by solvent environment, there has been a great deal of interest in understanding both static and dynamic solvent effects. The overall solvent dependence of absorption and emission spectra can be forecasted using continuum electrostatics and the Franck-Condon principle [14], especially when the influence of specific interactions (i.e., hydrogen bonding with explicit solvent molecules) is small. Onsager explained the underlying continuum electrostatic theory of a self-consistent solute-solvent “reaction field” for a polar molecule [15]. This model was further expanded with a slightly different assumption by considering the fluorophore to be a dipole in a continuous medium of uniform dielectric constant, and functions of the dielectric constant and refractive index were found to describe both polar and nonpolar solvent dependences of electronic spectra [16–19]. In addition, low-lying excited states associated with electron-donating or withdrawing substituents can cause large variations in the



Scheme 1 Structures of Cyclic Azacyanines (CACs 1–4)

photophysical and photochemical properties of molecules [20–22].

The majority of cyanine dyes, such as merocyanine dyes, show large solvatochromic shifts and second-order hyperpolarizabilities [23–25]. Several small carbocyanine dyes have shown interesting photophysical properties in non-polar solvents [26]. Various nonlinear optical experiments have led to different conclusions about the role of intramolecular interactions and solvent relaxation effects on the observed signals with tricarbocyanine dyes [27, 28]. In the past few decades, attention has been directed to the synthesis of cyclic azacyanines [29, 30] for various applications, including optical recording [31, 32]. Recently, we described solvatochromic

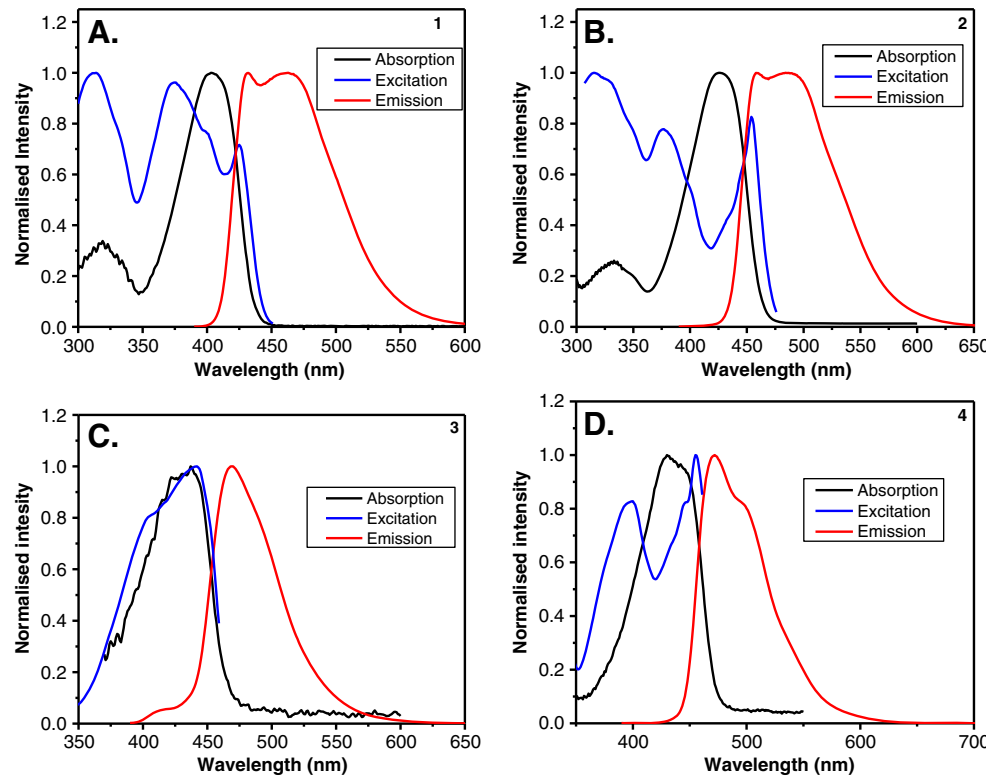
and substituent effects for a new class of sulfur containing CACs [1]. The objective of the present study is to establish the scope and limits of the influence of substituents on the optical dynamics and energy states of these underexplored compounds CACs 1–4 (see Scheme 1), as well as to study the apparent anomaly in the reaction of these CACs with hydroxide ion using Density Functional Theory (DFT). The results of steady state and time-resolved fluorescence measurements for several CAC molecules in various solvents as well as the results of quantum chemical calculations on their reactivity and spectral properties are presented.

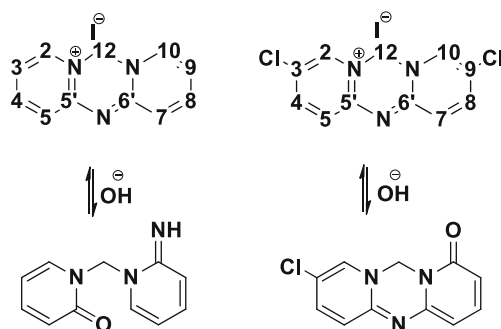
Results and Discussion

Spectroscopy

Figure 1 shows the UV-visible absorption, fluorescence excitation and emission spectra of 1–4 in water. The parent compound 1 showed a broad absorption in the wavelength region 350–450 nm ($S_0 - S_1$ transition), and another peak was observed in the region 300–350 nm ($S_0 - S_2$ transition). The spectral region for the $S_0 - S_1$ transition is similar to that obtained for S-containing CACs reported earlier [1], but the vibronic bands were not as well resolved in the present case. The absorption maximum for the $S_0 - S_1$ transition was found to be at 403 nm. However, the presence of electron withdrawing groups ($-Cl$ group as in 2) red-shifted the absorption

Fig. 1 Absorption, fluorescence excitation and emission spectra of cyclic azacyanine derivatives **a** 1, **b** 2, **c** 3 and, **d** 4 in water





Scheme 2 Reactivity of CACs during basic hydrolysis [30]

maximum 20 nm. This red shift is in accordance with the longer wavelength absorption of chlorobenzene compared to benzene ascribed to increased delocalization [33]. We propose that the red shift observed in the absorption spectra of 2 and 3 is due to π -donation into the cationic CAC π -system. Despite the fact that 2 possesses two apparent electron withdrawing groups (2,8-dichloro), its absorption spectrum exhibits a red shift, in analogy to 3, which possesses a more conventional electron donating group. It is known that halogens can act as π -donors in addition to being σ -withdrawing groups [34]. It is, therefore, expected that 3 should show a longer red shift (34 nm) than 2 (20 nm).

Unusual Reactivity

The regioselectivity of basic hydrolysis [30] of **2** is entirely different for the analogous reaction of **1** and **4** (Scheme 2). In the case of **1**, the hydroxide anion attacks the 5' position, but in the case of **2** the hydroxide anion appears to attack position 2 of the ring, leading to an oxo-product rather than the ring-opened product observed in the case of **1**. As the CACs are

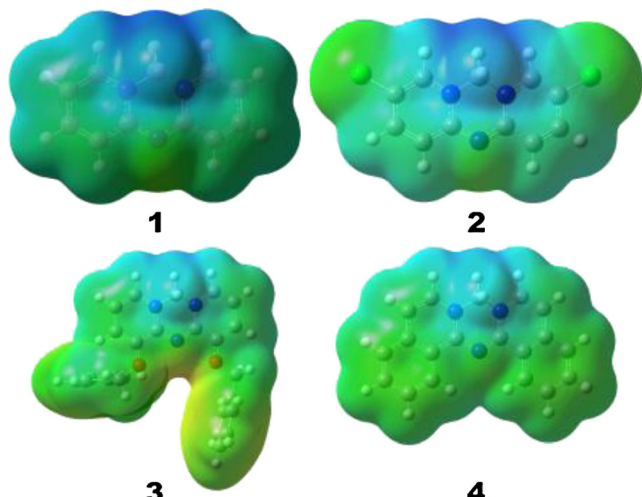


Fig. 2 Electrostatic potential maps of **1**, **2**, **3**, and **4** computed at M06-2X/6-31G+(d,p) in a solvent continuum of acetonitrile with a surface isovalue range of $-1.6e-2$ to $0.22e0$

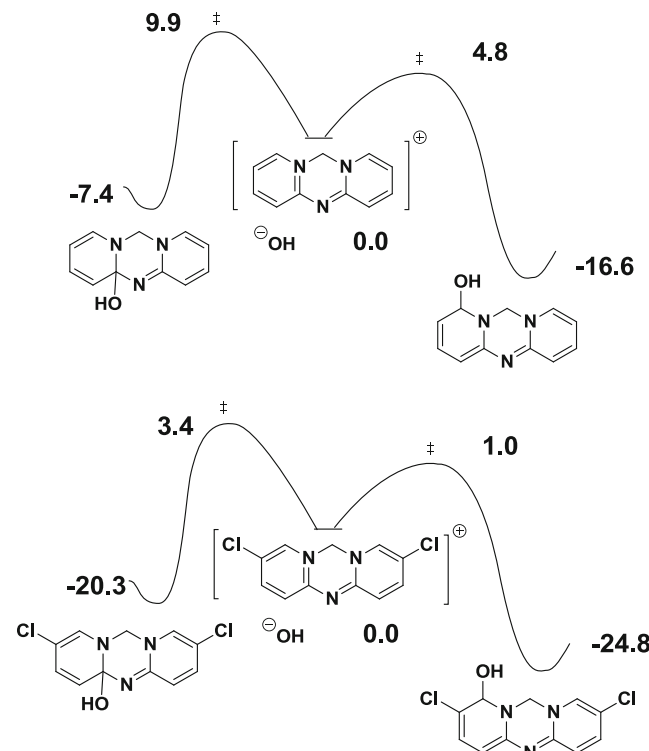
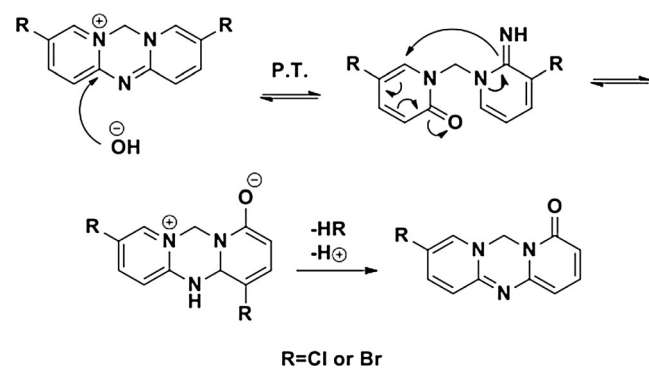


Fig. 3 Computational results for hydroxide addition to **1** and **2**. Relative energies shown in kcal/mol. Computed using M06-2X/6-31+G(d,p) in an SMD solvent model continuum of acetonitrile

cationic in solution, it is reasonable to assume that hydroxide anion attacks the position at which the cationic nature of the system is the greatest (due to resonance, σ -withdrawing effects, and/or other subtler electronic effects; assuming that steric effects do not overwhelm the electronic effects) so, electrostatic potential maps of **1–4** were generated. For all four structures, the largest concentration of partial positive charge is located on the aminal substructure of the central triazine ring (Fig. 2). With **1** (and **4**), hydroxide attack occurs at the tertiary fusion carbon (5') (Scheme 2) near to this region, although we would be hesitant to make a



Scheme 3 Proposed mechanism of amidine attack in a 1,6 fashion at the carbonyl of the ring system bearing substituent R

Table 1 Reactivity pathway calculations for **1**, **2**, and both mixed species performed at M06-2X and MPW1PW91 with a 6-31+G(d,p) basis set in an SMD solvent model continuum of methanol

CAC 1	M06 2X	MPW1PW91	CAC 2	M06 2X	MPW1PW91	CAC mix1	M06 2X	MPW1 PW91	CAC mix2	M06 2X	MPW1PW91
R	0	0	R	0	0	R	0	0	R	0	0
TS	20.5	18.8	TS	19.1	17.5	TS	22.0	20.1	TS	18.1	16.8
P	14.1	13.2	P	13.3	11.8	P	16.6	14.8	P	11.3	10.2

All energies presented in kcal/mol

R Reactant

TS Transition State

P Product

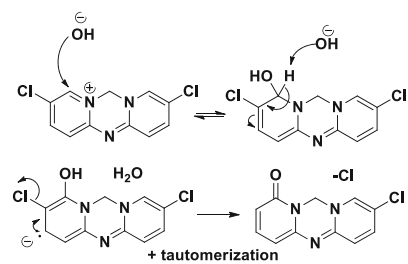
regioselectivity prediction on the basis of the electrostatic potential map alone. Conversely, with **2** we observe hydroxide attack at the carbon (2) that is adjacent to a fusion nitrogen and an additional σ withdrawing group—a Cl atom. This is also near to the concentrated region of positive charge. In **3**, we would expect to see the analogous oxo-product (as in **2**), but the reactivity of this system was not directly explored. Although hydroxide attack occurs near to the most positive region of the CACs, the observed regioselectivity is not easily predicted based on the charge distribution of the reactants alone.

In addition, the results of calculations on transition state structures for hydroxide attack (Fig. 3) do not predict the observed reactivity. For both **1** and **3**, attack at the 2-position is predicted. Taken together, our computed data on reactant and transition state structures for hydroxide attack are not consistent with rate-determining hydroxide addition, hinting that regioselectivity results from differences in subsequent mechanistic steps. With this in mind, we postulate that hydroxide attack occurs at the tertiary position in every case, but this attack is reversible. This then begs the question, if the initial hydroxide ion attack is not the rate determining step, what is? Although we have earlier [30] advanced a mechanism for the unusual **2**→**2a** conversion, we were ambivalent about this mechanism and now propose a more consistent approach to the reaction of these CACs with hydroxide ion. We propose that amidine attack is the rate determining step (Scheme 3). In **1** ($X_1 = X_2 = H$) the carbon that would be attacked by the imine is not electrophilic enough to undergo rapid 1,6 addition, whereas in **2** ($X_1 = X_2 = Cl$) the addition of the sigma withdrawing $-Cl$ increases the reactivity such that this 1,6 addition occurs. In addition, if this cyclization occurs it requires oxidation to give an analogue of **2a**; obviously the latter results from a predehydohalogenation step which is not possible for **1**. The case of **4** is similar to **1**, in that a 1,6-addition leads to an undesirable ortho-

quinoidal resonance contributing structure of the benzene ring.

Quantum chemical calculations on 1,6 attack were performed and the barrier for this attack, in the case of **1**, is predicted to be 1.3 kcal/mol higher than that for **2** (both relative to their respective reactants), consistent with the experimental evidence for this chemoselectivity. In addition to **1** and **2**, “mixed” (in which $X_1 = H$ and $X_2 = Cl$ and vice versa) species were analyzed computationally in an attempt to determine which ring system has a larger impact on the overall observed reactivity. The smallest barrier was predicted for $X_1 = Cl$ and $X_2 = H$, while the largest was predicted for $X_1 = H$ and $X_2 = H$. We extrapolate from this information, coupled with the experimental data, that the electron-withdrawing group at X_1 plays the larger role, since even when both X_1 and $X_2 = Cl$ the ring open product is not observed. The energies for all intermediates, transition state structures and zwitterionic products (before proton transfer) for **1**, **2**, and both mixed species are presented in Table 1.¹

¹ In the case of **CAC2** a benzyne intermediate can be envisaged which upon hydrolysis would lead to the observed product. Calculations performed on this intermediate eliminate it as a possibility for energetic reasons (see SI). The addition elimination mechanism shown here leading to the observed basic hydrolysis product of **CAC2** is also reasonable. We note that this is likely occurring in conjunction with our proposed pathway. In the case of **CAC1**, this addition elimination mechanism is not possible which is consistent with this reaction being under thermodynamic control as previously discussed.



Fluorescence Study

The fluorescence emission maximum of **1** was observed at 463 nm with two vibrational bands. The excitation spectrum of **1** indeed showed similar vibrational structures as did the emission spectrum, but was found to be different from the absorption spectrum. The difference in the excitation fluorescence and absorption spectra can be attributed to different species present in the excited and ground states, respectively. The Stokes shift given in Table 2 was computed to be 3,216 cm⁻¹.

The fluorescence maximum of **2** was red-shifted with similar vibrational bands as that of the parent **1**. It should be noted that the fluorescence spectrum of **3** is structured similarly to **1** and **2**. Conversely, the fluorescence

spectrum of **4** is more comparable to that of **3** than **1** or **2**. The shape of fluorescence excitation spectrum of **3** is quite similar to its absorption spectrum, unlike the case observed for **1** or **2** (See Fig. 1). These results are consistent with a model in which a π -electron-donating group ($-\text{OCH}_2\text{C}_6\text{H}_5$ in this case) delocalizes the positive charge on the **CAC** ring, favoring a planar structure. The fused benzene rings in **4** help to further delocalize the positive charge. The Stokes shifts of **3** and **4** are thus smaller than those of **1** and **2**. The fluorescence lifetime decay profile shown in Fig. 4 and data gathered in Table 2 also show longer lifetimes for **3** and **4** compared to **1** and **2**. We have also performed time-dependent (TD) DFT calculations to predict the absorbance spectra of this series of **CACs**. These calculations were performed using a variety of

Table 2 Spectroscopic parameters of **CAC 1–4**

Compound	Solvent	$\lambda_{\text{abs}}^{\text{max}}$ (nm)	$\lambda_{\text{em}}^{\text{max}}$ (nm)	Stokes shift (cm ⁻¹)	τ (ns)	χ^2
CAC 1	Acetonitrile	414	450	1932	2.93	1.25
	Water	403	463	3216	3.01	1.31
	Dichloromethane	425	448	1208	2.67	1.29
	DMF	416	449	1767	3.29	1.41
	DMSO	420	451	1637	3.37	1.29
	Ethanol	413	448	1892	3.09	1.21
	Methanol	412	458	2438	3.05	1.39
	N-Butyronitrile	422	447	1325	2.92	1.33
CAC 2	Acetonitrile	433	473	1953	2.49	1.77
	Water	426	484	2813	2.36	1.74
	Dichloromethane	449	476	1263	2.20	1.42
	DMF	436	480	2102	2.77	1.74
	DMSO	439	477	1815	2.74	1.41
	Ethanol	434	504	3200	2.58	1.59
	Methanol	433	493	2811	2.54	1.51
	N-Butyronitrile	435	478	2068	2.46	1.52
CAC 3	Acetonitrile	449	478	1351	5.41	1.33
	Water	437	469	1561	5.13	1.28
	Dichloromethane	453	482	1328	5.29	1.31
	DMF	452	482	1377	5.28	1.31
	DMSO	455	484	1317	5.30	1.46
	Ethanol	444	482	1776	5.45	1.34
	Methanol	442	479	1748	5.39	1.49
	N-Butyronitrile	449	480	1438	5.31	1.43
CAC 4	Acetonitrile	452	474	1027	5.76	1.78
	Water	430	472	2069	5.68	1.95
	Dichloromethane	454	475	974	5.06	1.94
	DMF	458	480	1001	5.42	1.41
	DMSO	462	483	941	4.70	1.33
	Ethanol	454	475	974	5.99	1.92
	Methanol	454	474	929	5.71	1.62
	N-Butyronitrile	455	475	925	5.31	1.39

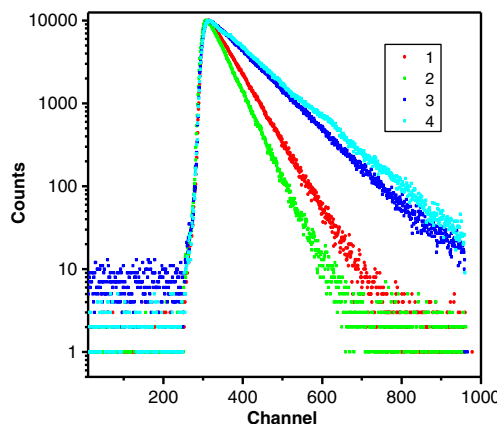


Fig. 4 Fluorescence lifetime decay profile of **1–4** in water

functionals [35–38], all with the 6-31+G(d,p) basis set in an SMD solvent continuum of acetonitrile (Table 3). Shifts in absorption maxima are well-reproduced, especially when using the B3LYP or PBE functionals in solvent. These methods therefore are likely to be useful in predicting spectra for other CACs not yet synthesized. Graphical overlays of the best computational and experimental data are shown in Fig. 6. For a complete description of all TD-DFT results for UV–vis data, see the Supporting Information.

Effect of Solvent Environments

To probe solvatochromic behavior, the absorption spectra of **1** were measured in various solvent environments. Measurements could not be made in hexane or cyclohexane due to poor solubility. The absorption spectra of **1** in various solvent environments are depicted in Fig. 5. These spectra display broad and intense absorptions in the 350 to 450 nm region; however, the spectral position is sensitive to the nature of the solvent. For example, the absorption maximum red-shifted from 403 nm in water to 425 nm in dichloromethane.

UV–vis calculations have been performed in dichloromethane, ethanol, and water in addition to acetonitrile for CACs **1–4**. It was found that the solvent effects observed experimentally are reproduced computationally at all three levels of theory previously discussed. The B3LYP functional proved the most advantageous for producing results closest in magnitude to the absolute value of the observed experimental λ_{\max} (Figs. 6 and 7) [39–41].² Since there is a substantial change in

the energy of transitions of **1** in different solvents, we propose that a polar solvent significantly stabilizes both the ground and excited state species. The fluorescence spectra of **1** were also found to be sensitive to solvent. It is important to note that the structure of the spectrum was more resolved in dichloromethane as compared to acetonitrile. While the absorption maximum was red shifted, the fluorescence maximum showed a blue shift from 463 nm in water to 448 nm in dichloromethane.

We propose that when the refractive index increases, the ground and excited states are both stabilized because of the movement of electrons within the solvent molecules. That is, an increase in refractive index facilitates movement of electrons within the solvent molecules and thus instantaneously stabilizes both the ground and excited states. As per the theory of general solvent effects [18, 19], this redistribution of electrons within the solvent molecules due to an increase in refractive index results in a decrease in the energy difference between the ground and excited states.

At the same time, the ground and excited states are also stabilized due to an increase in dielectric constant. However, the energy decrease of the excited state caused by the dielectric constant occurs only after reorientation of the solvent dipoles as this process necessitates movement of entire solvent molecules, not just electrons. Taking this into account, dielectric continuum theory describes environmental effects for which it is assumed that a point dipole solute interacts with the solvent by virtue of the change in solute dipole moment.

This change can be expressed by applying the Lippert–Mataga equation [18, 19] –

$$\overline{\nu_A} - \overline{\nu_F} = \frac{2}{hc} \left(\frac{\varepsilon - 1}{2\varepsilon + 1} - \frac{n^2 - 1}{2n^2 + 1} \right) \frac{(\mu_E - \mu_G)^2}{a^3} + \text{Constant}$$

– where $\overline{\nu_A}$ and $\overline{\nu_F}$ are the wave numbers (cm^{-1}) of the absorbance and fluorescence emission, respectively, h is Planck's constant, c is the speed of light in vacuum, a is the radius of the cavity in which the fluorophore resides, μ_E and μ_G are the dipole moments in the excited and ground states, respectively, and ε and n are the dielectric constant and the index of refraction of the solvents, respectively [19]. The Lippert–Mataga plot can be obtained by plotting the Stokes' shift versus the term in parentheses in the above equation (referred to as the orientation polarizability (Δf) of the solvent), which is the result of both the mobility of the electrons in the solvent and the dipole moment of the solvent.

$$(\Delta f) = \frac{\varepsilon - 1}{2\varepsilon + 1} - \frac{n^2 - 1}{2n^2 + 1}$$

² It is known that the B3LYP functional (when implemented in TD-DFT calculations) often overestimates absolute values of spectral features [39]. The M06-2X functional has been shown to be the safest choice for TD-DFT calculations [40] and as such was included in the set of functionals used herein (please see SI for complete details of all TD-DFT calculations). Previous studies of linear azacyanine dyes indicate that computing excited state geometry optimizations and relaxation energies can assist in obtaining more accurate data [41].

Table 3 Computational UV-vis data at varying levels of theory both in the gas phase and in a solvent continuum of acetonitrile (reported in nm)

Structure	λ_{\max} (exp., CH ₃ CN)	λ_{\max} (PBE)	λ_{\max} (B3LYP)	λ_{\max} (M06-2X)	λ_{\max} (PBE., CH ₃ CN)	λ_{\max} (B3LYP, CH ₃ CN)	λ_{\max} (M06-2X, CH ₃ CN)
1	414	365	372	356	369	376	358
2	433	390	398	375	388	396	373
3	449	401	409	388	402	409	389
4	452	394	403	375	407	416	386

The Lippert-Mataga plot of **1** in different solvents is presented in Fig. 5c. There are two kinds of linear correlations between the orientation polarizability of the solvent and Stokes' shift, with the difference between absorption and emission maxima obtained from the corrected spectra (on the wavenumber scale) of **1**. It is expected that the nitrogen atoms in **1** would interact specifically with protic solvents—like water, methanol and ethanol—by forming H-bonds. In the case of charge transfer in a molecule, the gross solvent polarity indicator scale, such as E_T (30), is more applicable [42]. E_T (30) is defined as the molar electronic transition energies (E_T) of dissolved pyridinium N-phenolate betaine dye in kcal/mol at STP [42]. A plot of the Stokes' shift of **1** versus the E_T (30) values of various solvents is given in Fig. 5d. In addition to specific solvent-fluorophore interaction, many molecules undergo internal charge transfer when a fluorophore contains both electron-accepting and donating groups. For example, the use of an amino group as an

electron donor and a carbonyl group as an electron-withdrawing group has been extensively examined and an increase in charge separation within the fluorophore is observed [43]. Since the parent chromophore of **1** has a positive charge localized in part on a nitrogen atom, charge separation is expected. Like the parent compound, broad absorption spectra were generally observed for substituted compounds **2–4**, as presented in Figs. 8, 9 and 10. The solvatochromic behavior of **2** was similar to that of **1**, but, in case of **3** and **4**, the plot of the Stokes shift vs E_T (30) gave two kinds of linear correlation for protic and aprotic solvent environments, respectively. This result is not surprising as the positive charge near to the nitrogen atom in **3** and **4** is further stabilized in the ground and excited states, as compared to **1** and **2**.

The fluorescence lifetime of **1** in various solvents showed mono exponential decay having a nanosecond fluorescence lifetime (refer to Table 1). The fluorescence lifetime is found to be in the same range reported earlier

Fig. 5 UV-Visible absorption (a), fluorescence emission (b) spectra of **1** in various solvents of different polarity. c Lippert Mataga plot for **1** in various solvents showing the variation of Stokes' shift as a function of orientation polarizability of the solvents. d Correlation of Stokes shift of **1** with E_T (30) parameter in various solvents

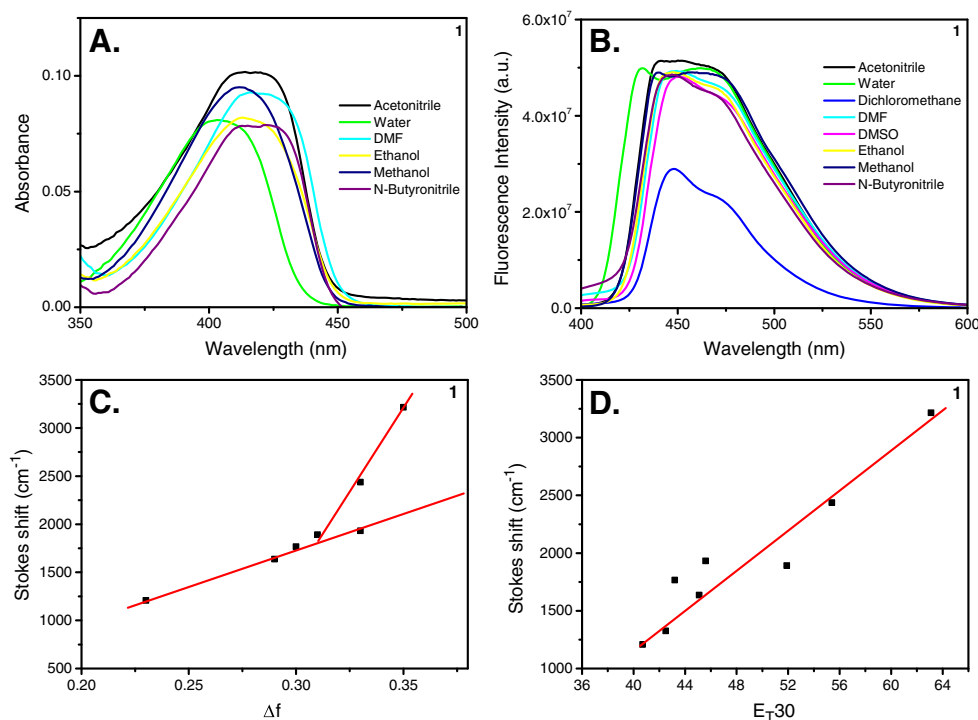
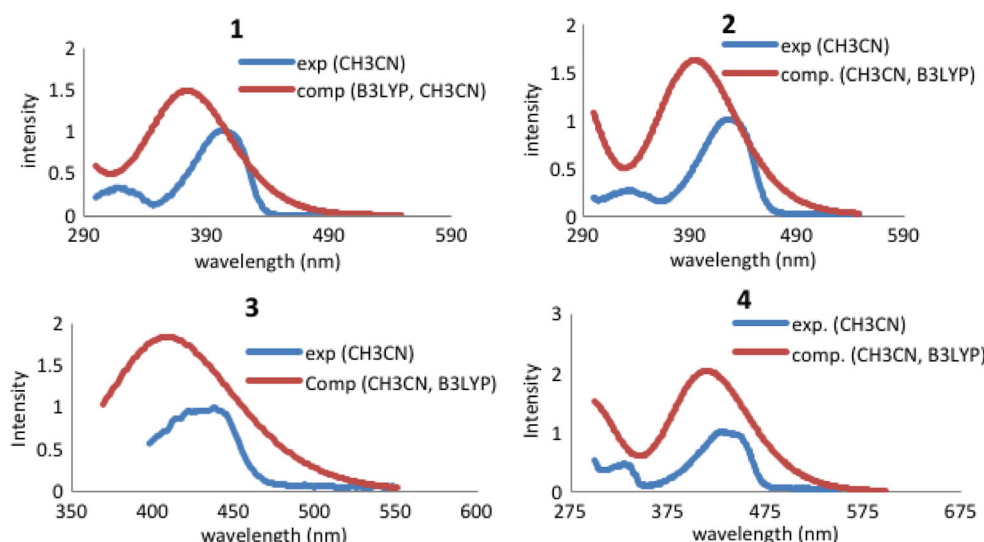


Fig. 6 Experimental and computational UV-vis spectral overlays: experimental spectra in acetonitrile and computational data performed using B3LYP/6-31+G(d,p) in a solvent model continuum of acetonitrile



for S-containing **CACs** [1], which is longer than for some merocyanine dyes [44], Cy3 [45] and Cy5 [46] but shorter than polymethine dyes [47]. The excited state lifetime values were highest in polar solvents like DMF and DMSO; it is thought that polar solvents stabilize the excited states, thereby increasing the fluorescence lifetimes.

The slight decrease in fluorescence lifetime in ethanol, methanol and water could be due to specific H-bonding interactions. The relatively short lifetimes of **1** in dichloromethane can be attributed to decreased stabilization of the excited state in less polar solvents. The excited state fluorescence lifetime of **2** was generally found to be shorter than that of **1**.

This could be due to increased constraint in the excited state of **2** compared to **1**. On the other hand the excited state lifetime of **3** was enhanced remarkably compared to **1** (in some cases a >70 % increase as compared to **1** and more than two fold relative to **2**). These longer lifetimes for **3** indicate that the excited state is stabilized due to the presence of an electron-donating group. The excited state lifetime values obtained for **4** were similar to those of **3**.

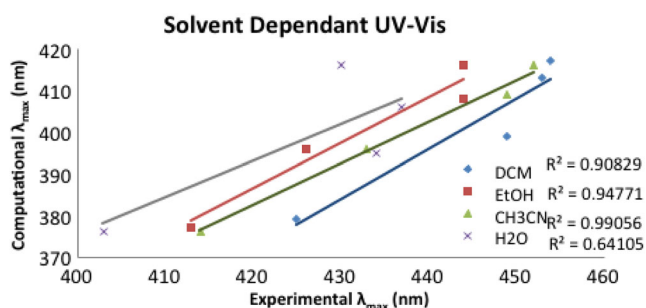


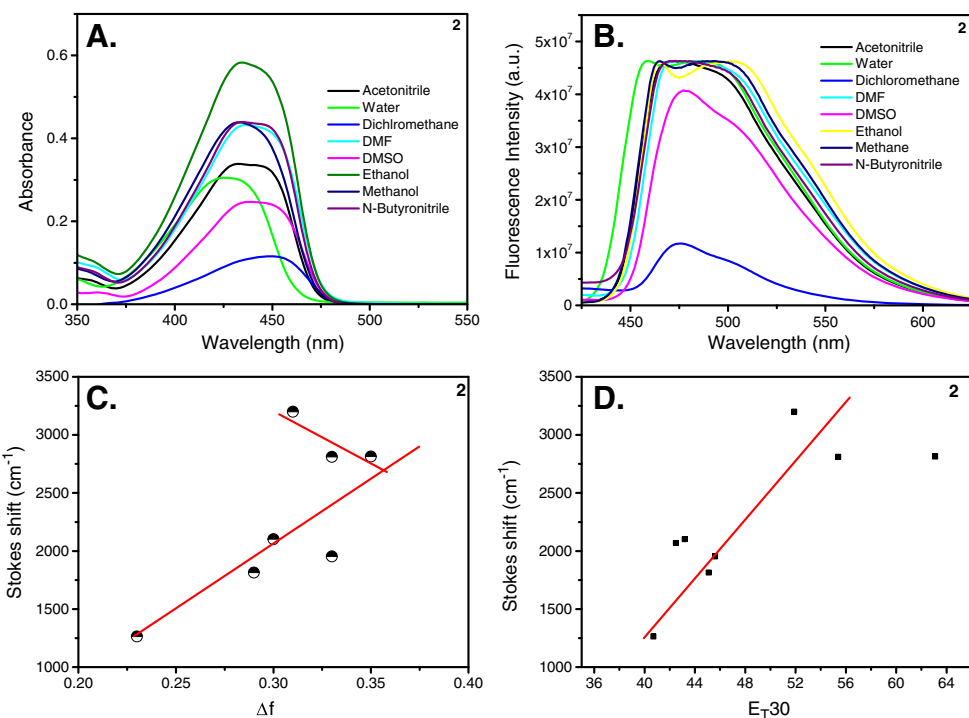
Fig. 7 Solvent dependent TD-DFT UV-vis calculations performed using B3LYP/6-31G+(d,p) in SMD solvent continuum models of dichloromethane, ethanol, acetonitrile, and water respectively on structures optimized using M06-2X/6-31G+(d,p) in the gas phase

and, in general, a slightly higher value for **4** compared to **3** could be due to increased delocalization. These results suggest potential applications of these classes of cyclic azacyanines as solvatochromic probes for use in single molecule fluorescence studies and, potentially, for use in biophysical and biomedical assays.

Conclusions

Absorption, steady-state and lifetime of fluorescence investigations of several cyclic azacyanines were carried out in various solvent environments. It was found that introduction of electron-donating/withdrawing groups on the **CAC** modulated the spectroscopic properties. Although this work builds on our previous work [30], new spectroscopic data and DFT calculations are described (the latter clarifies previous assumptions). Unlike in the parent compound, introduction of an electron donating group (**3**) appears to encourage similar structures in the ground and excited states by stabilizing the positive charge on the ring of the **CAC**. Interestingly, introduction of an electron-withdrawing group (**2**) also appears to stabilize the positive charge as a similar red shift in the fluorescence was observed relative to **3**. **CACs** display solvent dependent relaxation; in protic solvents, specific interactions of solvent molecules further enhance this effect. Fluorescence lifetime decay indicates a relaxation period on the nanosecond timescale with monoexponential decay; the fluorescence lifetime values are in the same range found earlier for another class of **CACs** [1]. Electron-donating substituents (as in **2**) extend the excited state lifetime, whereas electron-withdrawing groups (as in **3**) marginally decrease the excited state lifetime compared to

Fig. 8 UV-Visible absorption (a), fluorescence emission (b) spectra of **2** in various solvents of different polarity. **c** Lippert Mataga plot for **2** in various solvents showing the variation of Stokes' shift as a function of orientation polarizability of the solvents. **d** Correlation of Stokes shift of **2** with $E_T(30)$ parameter in various solvents



that of the parent compound (**1**). TD-DFT was used to predict the absorption maxima of this class of compounds and a useful model for predicting spectroscopic characteristics of similar compounds has emerged. Finally, the regioselectivity of basic hydrolysis was studied using

quantum chemical calculations, which predict that 1,6 addition to a carbonyl is the rate and product determining (i.e. ring-opened or closed) step. The results described herein point to potential applications of cyclic azacyanines as solvatochromic probes for biomedical

Fig. 9 UV-Visible absorption (a), fluorescence emission (b) spectra of **3** in various solvents of different polarity. **c** Lippert Mataga plot for **3** in various solvents showing the variation of Stokes' shift as a function of orientation polarizability of the solvents. **d** Correlation of Stokes shift of **3** with $E_T(30)$ parameter in various solvents

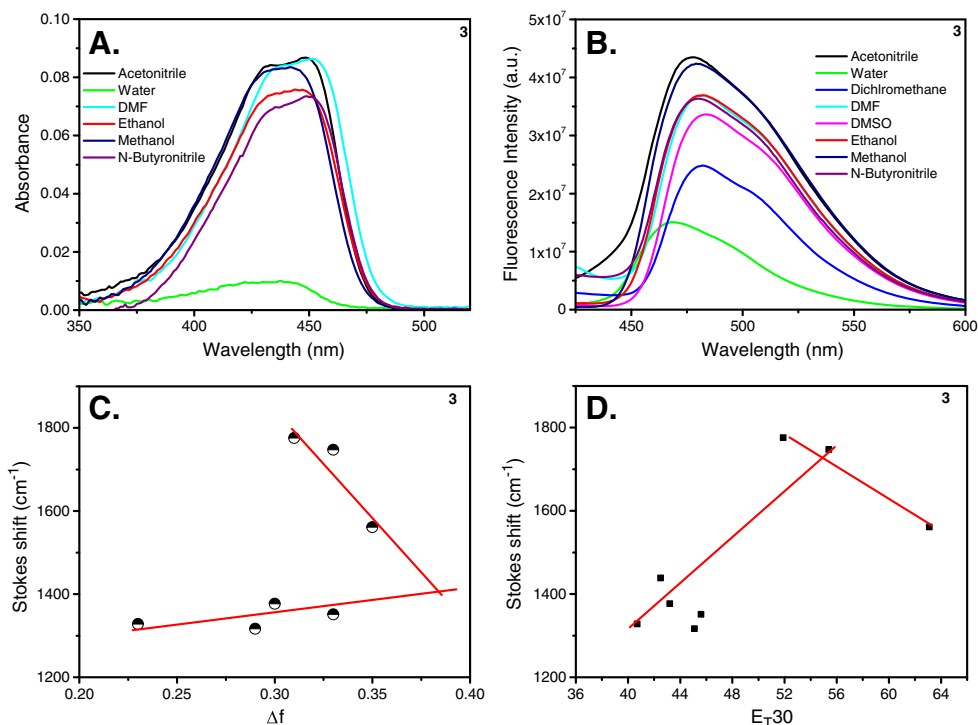
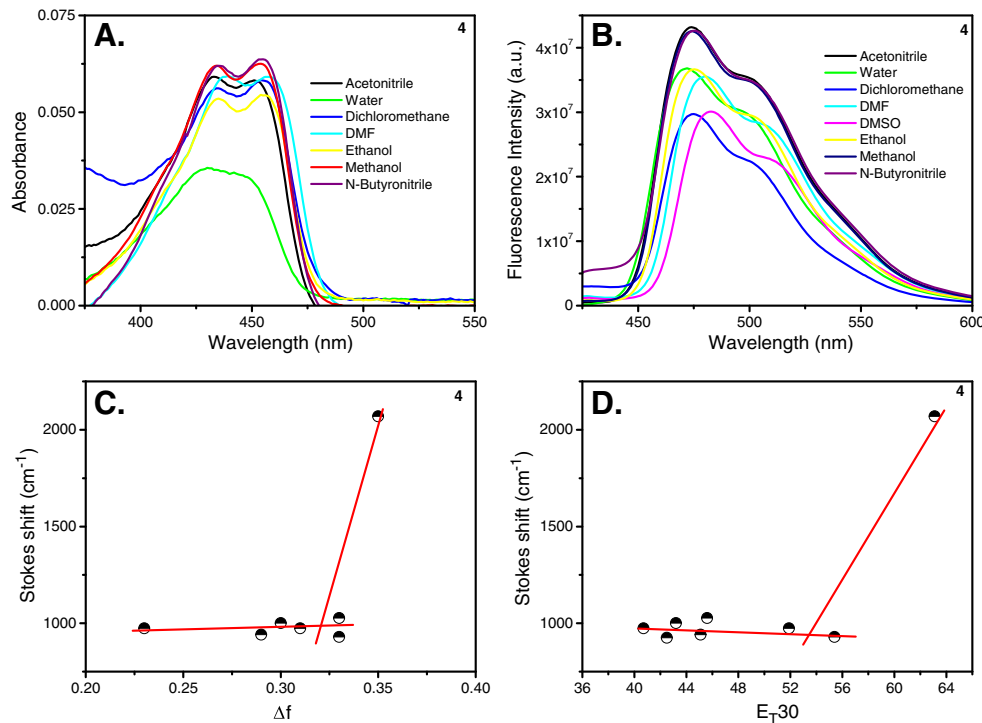


Fig. 10 UV-Visible absorption (**a**), fluorescence emission (**b**) spectra of **4** in various solvents of different polarity. **c** Lippert Mataga plot for **4** in various solvents showing the variation of Stokes' shift as a function of orientation polarizability of the solvents. **d** Correlation of Stokes shift of **4** with $E_T(30)$ parameter in various solvents



assays, single molecule fluorescence studies, investigations concerning solvation dynamics. In addition, quantum chemical calculations of the type described herein may prove useful for the design of new fluorophores.

Experimental Section

Synthesis

The syntheses of CAC derivatives, **1–4** (see Scheme 1), were carried out via the one-step reaction of an α -amino-substituted heterocycle with diiodomethane. The detailed synthetic procedure and characterization of these compounds has been reported elsewhere [29, 30]. For basic hydrolysis, the cyclic azacyanine and its derivatives, **1–4**, were reacted with hydroxide ions (10 % methanolic KOH solution) at room temperature [30].

Materials

To prepare the stock solution, CACs were dissolved in spectroscopic grade dichloromethane. A desired amount of the stock solution was transferred to a vial and the solvent evaporated via gentle heating. The final sample solution was prepared by adding the required amount of the desired solvent into the same vial. Ethanol, methanol, acetonitrile, n-butyronitrile (nBN), and N,N-dimethylformamide (DMF) were of spectroscopy grade and were used without further purification.

Spectroscopic Measurements

The absorption spectra in various solvents were recorded at room temperature using a JASCO V-570 UV–VIS-NIR Spectrophotometer. Fluorescence measurements were done on a JOBIN YVON Horiba Fluorolog 3 spectrofluorometer. The excitation source was a 100 W Xenon lamp. The detector used was an R-928 operating at a voltage of 950 V. The excitation and emission slits width were 5 nm. The spectral data were collected using Fluorescence software and data analysis was conducted using OriginPro 6.0 software. Fluorescence lifetime measurements were done using the same instrument but coupled with a pulsed diode laser. A 405 nm diode laser was used as the excitation source and the detector used was an R-928 operating at a voltage of 950 V. The fluorescence decay was acquired with a peak preset of 10,000 counts and the decay data were analyzed using data analysis software provided with the instrumentation.

Computational Methods

All calculations were performed in Gaussian09 [48] using DFT. The M06-2X [49] functional and a 6-31+G(d,p) basis set were used unless otherwise stated. Electrostatic potential maps were created using Gaussview with an isovalue range of $-1.6\text{e-}2$ to $0.220\text{e}0$ and an un-faded transparent surface. All optimized structures were verified as minima or transition state structures using frequency calculations (no imaginary frequencies or one imaginary frequency, respectively). In some cases, solvent was included using the SMD continuum

model [50]. All time-dependent calculations were performed using *nstates* = 20 and *root* = 1 [51] commands with a 6-31+G(d,p) basis set (and a variety of functionals as described in the text) using the SMD continuum model for acetonitrile solvation. Energies, coordinates, and normal mode analysis for all structures, as well as TD-DFT results, are available in the [Supporting Information](#).

Acknowledgments The authors thank American University of Beirut through its University Research Board (URB) and the NSF XSEDE program (CHE-030089) for financial support. We thank Professor Bilal Kaafarani, who made valuable comments on this manuscript.

References

- Patra D, Malaeb NM, Haddadin MJ (2012) Influence of substituent and solvent on the radiative process of singlet excited states of novel cyclic azacyanine derivatives. *J Fluoresc* 22:707–717
- Behera GB, Behera PK, Mishra BK (2007) Cyanine dyes: self aggregation and behaviour in surfactants: a review. *J Surf Sci Technol* 23:1–31
- Doja MQ (1932) The cyanine dyes. *Chem Rev* 11:273–321
- Mishra A, Behera RK, Behera PK, Mishra BK, Behera GB (2000) Cyanine dyes during the nineties: a review. *Chem Rev* 100:1973–2011
- Mujumdar RB, Ernst LA, Mujumdar SR, Lewis CJ, Waggoner AS (1993) Cyanine dye labeling reagents: sulfoindocyanine succinimidyl esters. *Bioconjug Chem* 4:105–111
- Ernst LA, Gupta RK, Mujumdar RB, Waggoner AS (1989) Cyanine dye labeling reagents for sulfhydryl groups. *Cytometry* 10:3–10
- Blower MD, Feric E, Weis K, Heald R (2007) Genome-wide analysis demonstrates conserved localization of messenger RNAs to mitotic microtubules. *J Cell Biol* 179:1365–1373
- Patra D (2008) Application and developments in fluorescence spectroscopic techniques in studying individual molecules. *Appl Spectrosc Rev* 43:389–415
- Patra D (2008) Single molecule studies in chemical biology and nanosciences. *Curr Chem Biol* 2:267–277
- Singh MK (2009) Time-resolved single molecule fluorescence spectroscopy of Cy5-dCTP: influence of the immobilization strategy. *Phys Chem Chem Phys* 11:7225–7230
- Deniz AA, Laurence TA, Beligere GS, Dahan M, Martin AB, Chemla DS, Dawson PE, Schultz PG, Weiss S (2000) Single-molecule protein folding: diffusion fluorescence resonance energy transfer studies of the denaturation of chymotrypsin inhibitor 2. *Proc Natl Acad Sci U S A* 97:5179–5184
- Enderlein J, Gregor I, Patra D, Fitter J (2005) Statistical analysis of diffusion coefficient determination by fluorescence correlation spectroscopy. *J Fluoresc* 15:415–422
- McHale JL (2001) Subpicosecond solvent dynamics in charge-transfer transitions: challenges and opportunities in resonance Raman spectroscopy. *Acc Chem Res* 34:265–272
- Bayliss NSJ (1950) The effect of the electrostatic polarization of the solvent on electronic absorption spectra in solution. *J Chem Phys* 18: 292–296
- Onsager L (1936) Electric moments of molecules in liquids. *J Am Chem Soc* 58:1486–1493
- Mataga N, Kubota T (1970) Molecular interactions of electronic spectra. Marcel Dekker, New York
- Liptay W (1974) Dipole moments and polarizabilities of molecules in excited electronic states. In: Lim EC (ed) *Excited states*, vol I. Academic, New York, p 129–229
- Patra D, Barakat C (2011) Synchronous fluorescence spectroscopic study of solvatochromic curcumin dye. *Spectrochim Acta A* 79: 1034–1042
- Lakowicz JR (1999) *Principles of fluorescence spectroscopy*. Kluwer Academic, Plenum Publishers, New York
- Tolbert LM, Nesselroth SM, Netzel TL, Raya N, Stapletons M (1992) Substituent effects on carbanion photophysics 9-arylfluorenlyl anions. *J Phys Chem* 96:4492–4496
- Turro N (1978) *Modern molecular photochemistry*. Benjamin Cummings, New York
- Wagner PJ, Siebert EJ (1981) Deactivation of triplet phenyl alkyl ketones by conjugatively electron-withdrawing substituents. *J Am Chem Soc* 103:7329–7335
- Brooker LGC, Keyes GH, Sprague RH, Van Dyke RH, VanLare E, Vanzandt G, White FL, Cressman HWJ, Dent SG (1951) Studies in the cyanine dye series. XI. The mercocyanines. *J Am Chem Soc* 73: 5326–5332
- Valenzano DP (1987) Photomodification of biological membranes with emphasis on singlet oxygen mechanisms. *Photochem Photobiol* 47:147–160
- Panigrahi M, Dash S, Patel S, Mishra BK (2011) Preferential solvation of styrylpyridinium dyes in binary mixtures of alcohols with hexane, dioxane, and dichloromethane. *J Phys Chem B* 115:99–108
- West W, Geddes AL (1964) The effects of solvents and of solid substrates on the visible molecular absorption spectrum of cyanine dyes. *J Phys Chem* 68:837–847
- Cong P, Yan YJ, Deuel HP, Simon JD (1994) Non-Markovian optical dephasing dynamics in room temperature liquids investigated by femtosecond transient absorption spectroscopy: theory and experiment. *J Chem Phys* 100:7855–7866
- Yang T-S, Vöhringer P, Arnett DC, Scherer NF (1995) The solvent spectral density and vibrational multimode approach to optical dephasing: two-pulse photon echo response. *J Chem Phys* 103: 8346–8359
- Haddadin MJ, Kurth MJ, Olmstead MM (2000) One-step synthesis of new heterocyclic azacyanines. *Tetrahedron Lett* 41:5613–5616
- Huang KS, Haddadin MJ, Olmstead MM, Kurth MJ (2001) Synthesis and reaction of some heterocyclic azacyanines. *J Org Chem* 66:1310–1315
- Kurose Y, Miyazawa T, Kubo H, Uchida N, Furomoto S, Satake K, Shoda H, Aizawa Y, Dan-Oh Y, Toki M (2007) Optical recording medium and azacyanine dye. *PCT Int Appl*. WO 2007074861 A1 20070705
- Griffiths J, Li Z (1993) Azacyanine dyes with acridinium terminal groups- a new series of near infrared absorbing dyes. *Dyes Pigments* 21:205–216
- Forbes WF (1960) Light absorption studies. Part XVII. The ultraviolet absorption spectra of chlorobenzenes. *Can J Chem* 38:1104–1112
- Housecroft CE, Sharpe AG (2008) *Inorganic chemistry*, 3rd edn. Pearson Education Limited, Upper Saddle River, Ch. 21
- Perdew JP, Burke K, Erzenhoff M (1996) Generalized gradient approximation made simple. *Phys Rev Lett* 77:3865–3868
- Becke AD (1993) A new mixing of Hartree-Fock and local density-functional theories. *J Chem Phys* 98:1372–1377
- Becke AD (1993) Density functional thermochemistry. III. The role of exact exchange. *J Chem Phys* 98:5648–5652
- Lee C, Yang W, Parr RG (1988) Development of the Colle-Salvetti correlation-energy formula into a functional of the electron density. *Phys Rev B* 37:785–789
- Moore B II, Autschbach J (2013) Longest-wavelength electronic excitations of linear ... and of approximations in time-dependent density functional theory. *J Chem Theory Comput* 9:4991–5003

40. Jacquemin D, Zhao Y, Valero R, Adamo C, Ciofini I, Truhlar DG (2012) Verdict: time-dependent density functional theory “not guilty” of large errors for cyanines. *J Chem Theory Comput* 8:1255–1259

41. Send R, Valsson O, Filippi C (2011) Electronic excitations of simple cyanine dyes: reconciling density functional and wave functional methods. *J Chem Theory Comput* 7:444–455

42. Reichardt C (1994) Solvatochromic dyes as solvent polarity indicators. *Chem Rev* 94:2319–2358

43. Kon H, Szent-Gyorgyi A (1973) Charge transfer between amine and carbonyl. *Proc Natl Acad Sci U S A* 70(11):3139–3140

44. Mishra A, Behera GB, Krishna MMG, Periasamy N (2001) Time-resolved fluorescence studies of aminostyryl pyridinium dyes in organic solvents and surfactant solutions. *J Lumin* 92:175–188

45. Sanborn ME, Connolly BK, Gurunathan K, Levitus M (2007) Fluorescence properties and photophysics of the sulfoindocyanine Cy3 linked covalently to DNA. *J Phys Chem B* 111:11064–11074

46. Huang Z, Ji D, Xia A (2005) Fluorescence intensity and lifetime fluctuation of single Cy5 molecules immobilized on the glass surface. *Colloids Surf A Physicochem Eng* 257–258: 203–209

47. Demchuk MI, Ishchenko AA, Krasnaya ZA, Mikhailov VP (1990) The excited-state relaxation times of cationic-anionic polymethine dyes. *Chem Phys Lett* 167:170–174

48. Frisch MJ (2010) Gaussian 09, Revision B.01. Gaussian, Inc, Wallingford, Full reference in Supporting Information

49. Zhao Y, Truhlar DG (2007) The M06 suite of density functionals for main group thermochemistry, kinetics, noncovalent interactions, excited states, and transition elements: two new functionals and systematic testing of four M06 functionals and twelve other functionals. *Theor Chem Accounts* 120:215–241

50. Marenich AV, Cramer CJ, Truhlar DG (2009) Universal solvation model based on solute electron density and continuum model of the solvent defined by the bulk dielectric constant and atomic surface tensions. *J Phys Chem B* 113:6378–6396

51. Bauernschmitt R, Alrichs R (1996) Treatment of electronic excitations within the adiabatic approximation of time dependent density functional theory. *Chem Phys Lett* 256:454–464